Supporting Information

The kinetics enhancement of hierarchical hollow boride microsphere for double-high aqueous Zn-based battery

Shiyu Gu[1,3,&], Yaqi Wu[1,3,&], Liyuan Liu[1], Yang Li[1], Zihan Yang[1], Xiaodan Xia[1,2], Jinling Zhao[1,2], Qingliang Lv[1,4], Dehong Chen[1,*], Zhenyu Xiao[1,*]

[1] Key Laboratory of Eco-chemical Engineering, Ministry of Education, International Science and Technology Cooperation Base of Eco-chemical Engineering and Green Manufacturing, College of Chemistry and Molecular Engineering, Qingdao University of Science and Technology, Qingdao 266042, P. R. China.

[2] Qingdao Haifa State Owned Capital Investment and Operation Group Co., Ltd., Qingdao 266431, P. R. China.

[3] Shandong Engineering Research Center for Marine Environment Corrosion and Safety Protection, College of Environment and Safety Engineering, Qingdao University of Science and Technology, Qingdao 266042, P. R. China.

[4] Chemical Engineering Institute, Qingdao University of Science and Technology, Qingdao 266042, P. R. China.

[&] These authors contributed equally to this work and should be considered co-first authors.

Characterization

The morphology of the CNB hollow polyhedron structures is investigated with scanning electron microscopy (SEM, Zeiss merlin) and transmission electron microscopy (TEM, FEI Tecnai G2 F20). The X-ray diffraction (XRD) patterns of the samples are recorded on a Rigaku D-MAX2500/PC advance instrument with Cu-Kα radiation (λ ¼ 1.5418 Å). The X-ray photoelectron spectroscopy (XPS) is measured on by thermo Scientific 250xl, and the thermogravimetric analysis (TGA) is tested by TA SDT Q600.

Figure:

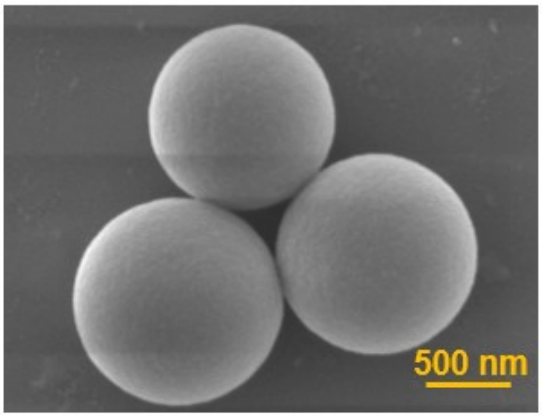

Figure S1. The SEM of Co_3/Ni_7-BTC precursor samples.

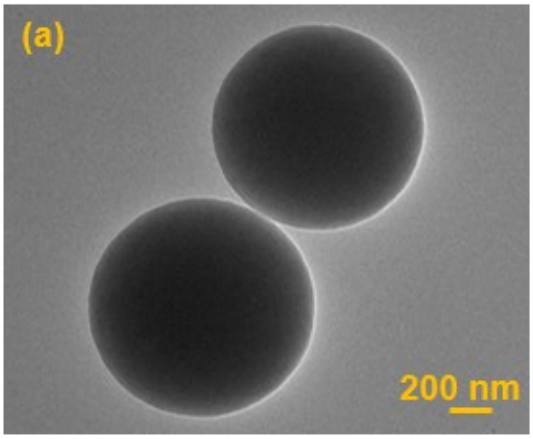

Figure S2. The SEM of Co_3/Ni_7-BTC precursor samples.

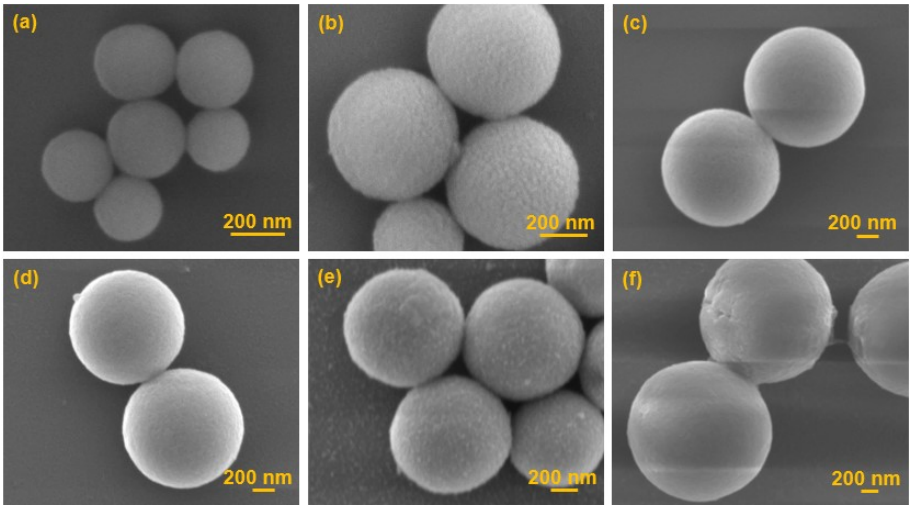

Figure S3. The SEM of different precursors synthesized according to different ratios of cobalt and nickel, (a) Ni-BTC; (b) Co_1/Ni_9-BTC; (c) Co_2/Ni_8-BTC; (d) Co_4/Ni_6-BTC; (e) Co_5/Ni_5-BTC; (f) Co-BTC.

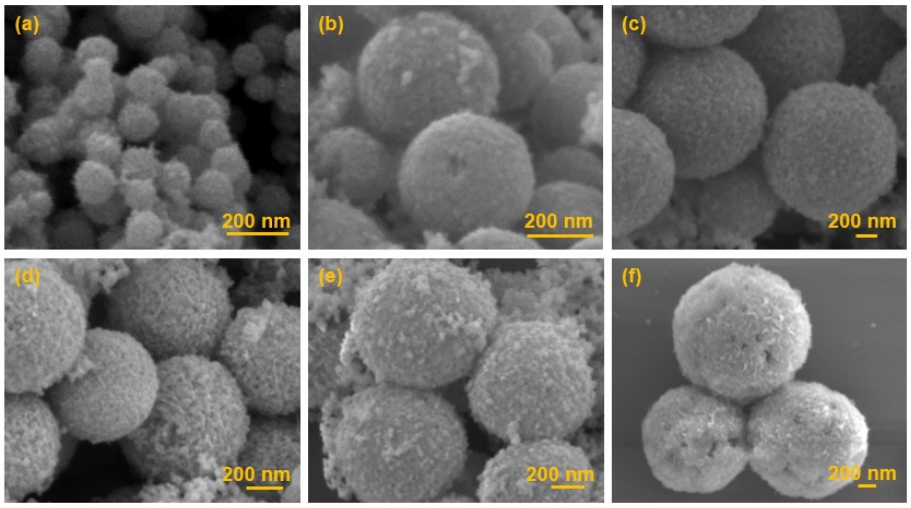

Figure S4. The SEM of (a) NB; (b) C_1N_9B; (c) C_2N_8B; (d) C_4N_6B; (e) C_5N_5B; (f) CB.

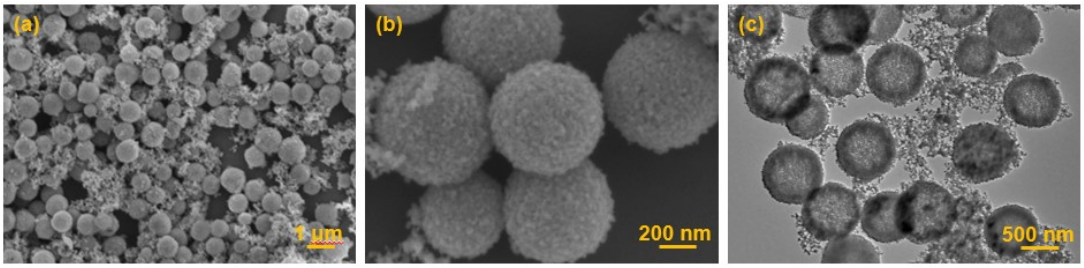

Figure S5. (a) - (b) The SEM of CNB sample; (c) The TEM of CNB sample.

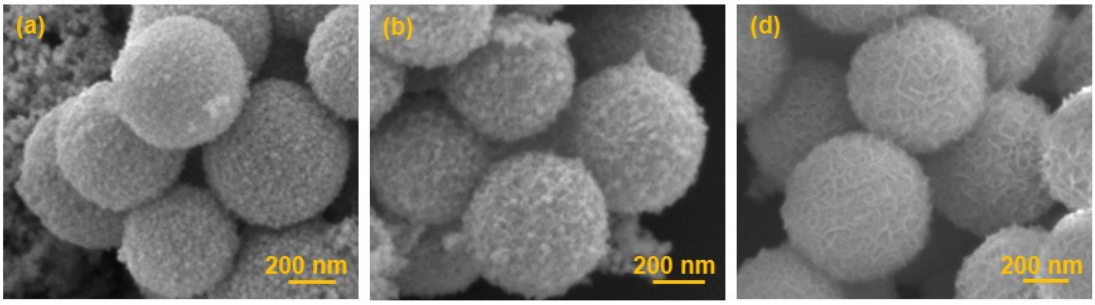

Figure S6. The SEM of (a) CNB-15 min; (b) CNB-60 min; (c) CNB-90 min.

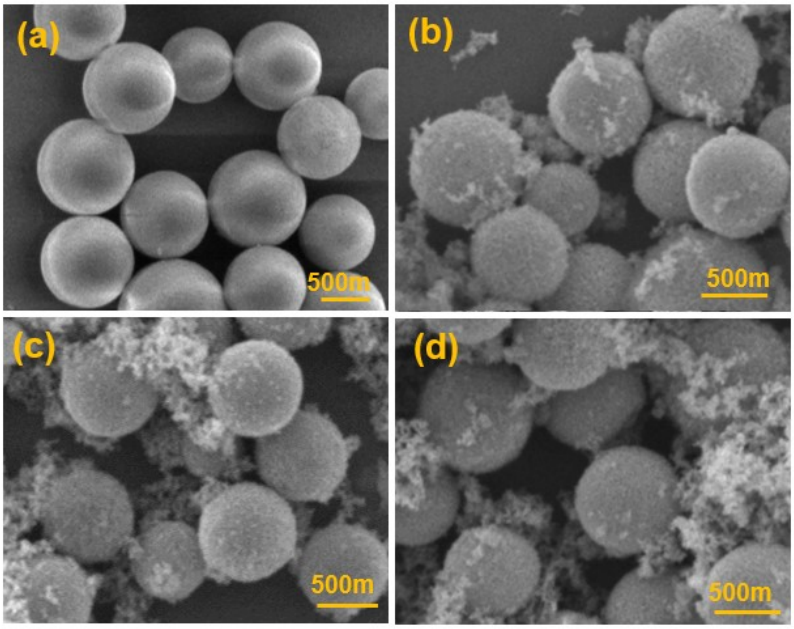

Figure S7. The SEM of (a) CNB-0 M; (b) CNB-0.2 M; (c) CNB-0.6 M; (d) CNB-0.8 M.

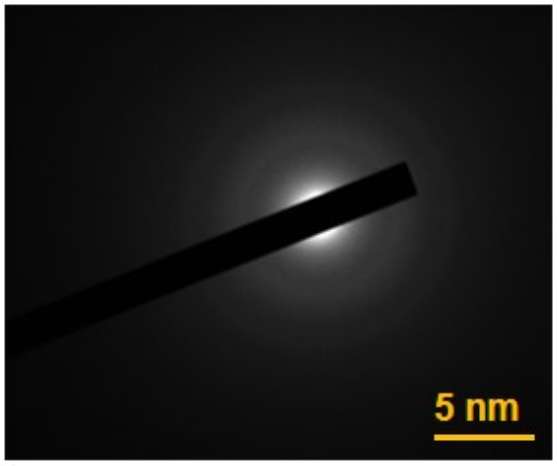

Figure S8. Selected area electron diffraction (SAED) pattern of the CNB.

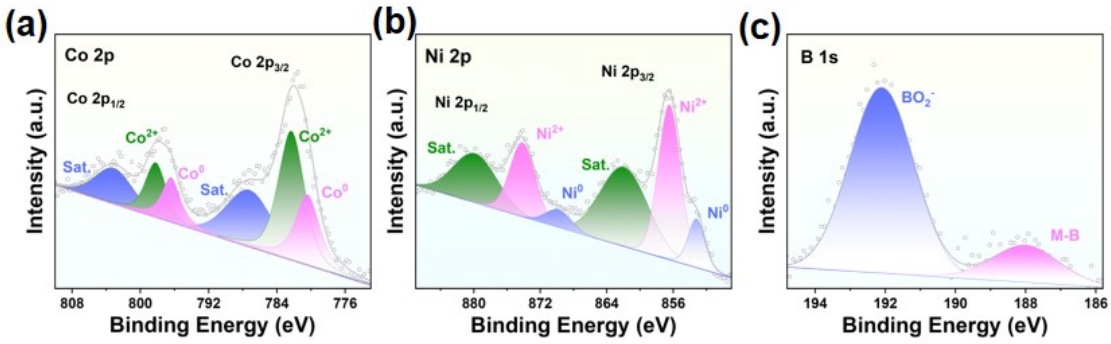

Figure S9. The XPS spectra of (a) Co 2p; (b) Ni 2p; and (c) B 1s of CNB.

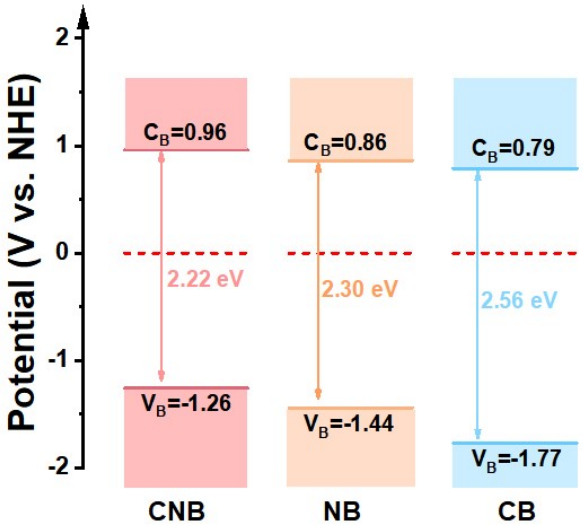

Figure S10. The energy band diagram of CNB, NB, and CB.

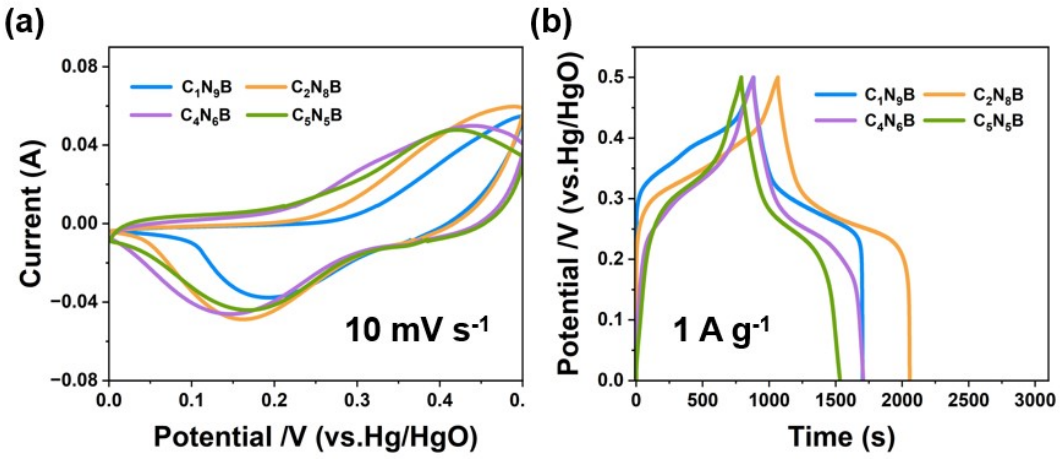

Figure S11. The (a) CV curves and (b) GCD curves of C_1N_9B, C_2N_8B, C_4N_6B and C_5N_5B.

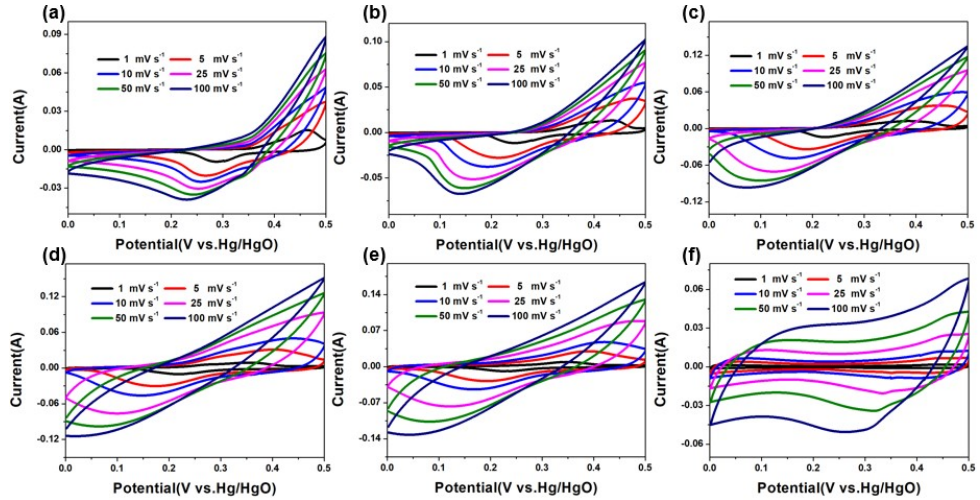

Figure S12. The CV curves of (a) NB; (b) C_1N_9B; (c) C_2N_8B; (d) C_4N_6B; (e) C_5N_5B; (f) CB.

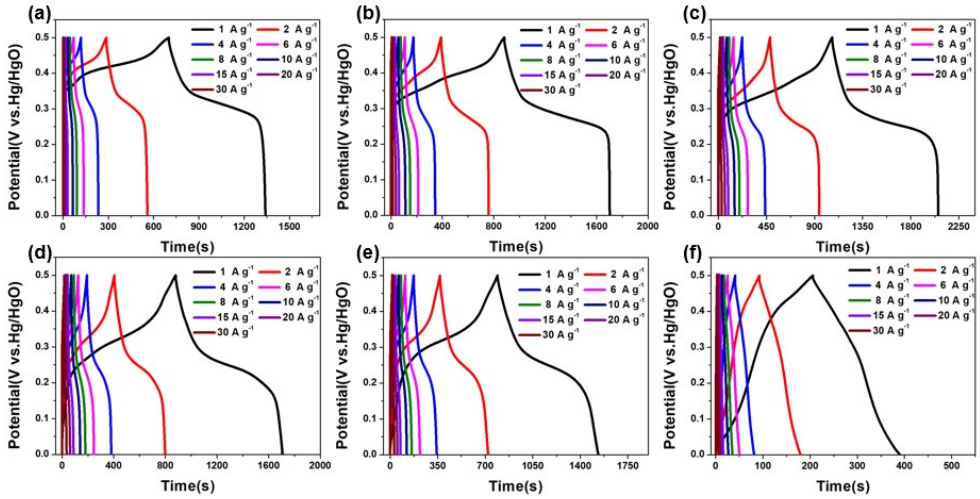

Figure S13. The GCD curves of (a) NB; (b) C_1N_9B; (c) C_2N_8B; (d) C_4N_6B; (e) C_5N_5B; (f) CB.

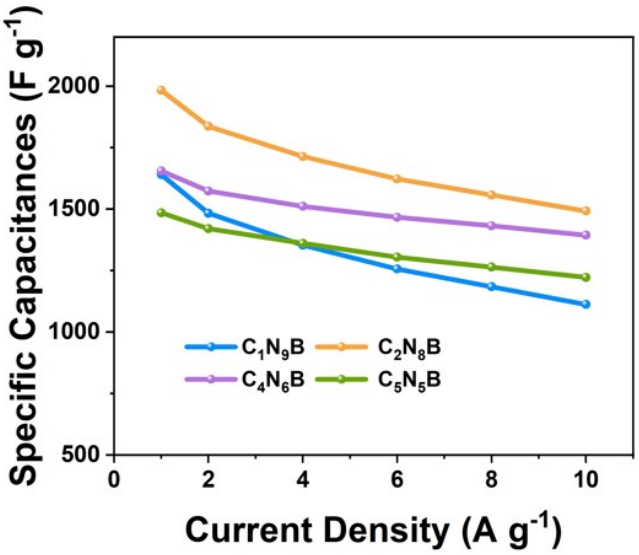

Figure S14. The specific capacitance at different charge/discharge current densities of C_1N_9B, C_2N_8B, C_4N_6B and C_5N_5B.

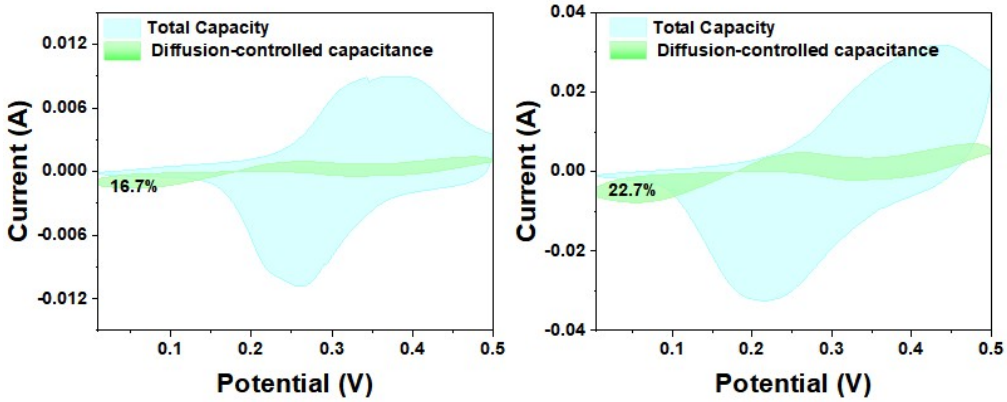

Figure S15. The capacitive contribution at a scan rate of 1.0 mV s^{-1} and 5.0 mV s^{-1}.

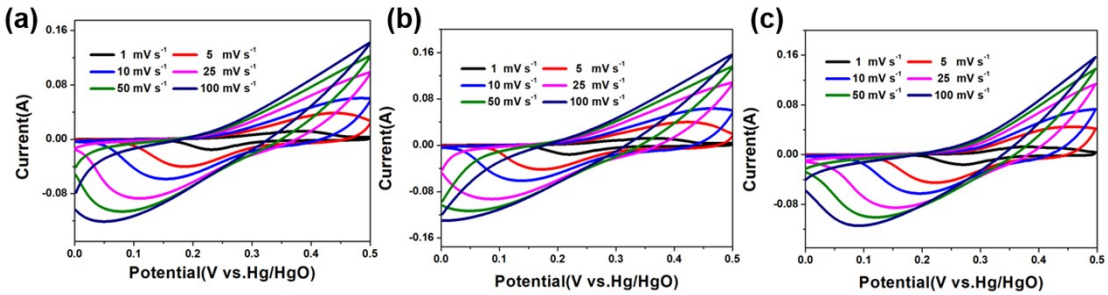

Figure S16. The CV curves of (a) CNB-15 min; (b) CNB-60 min; (c) CNB-90 min.

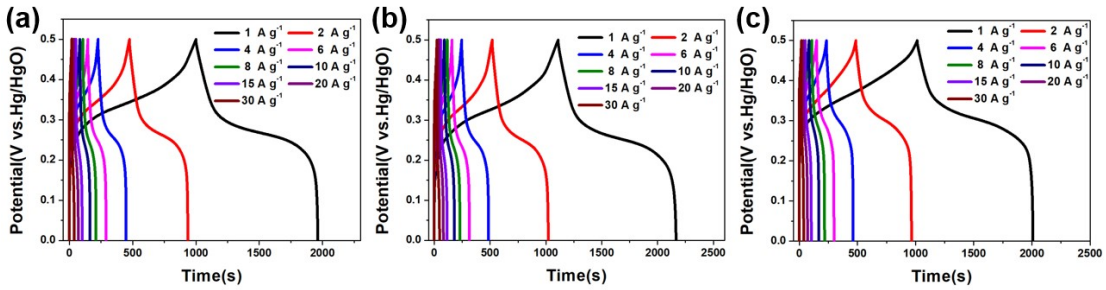

Figure S17. The GCD curves of (a) CNB-15 min; (b) CNB-60 min; (c) CNB-90 min.

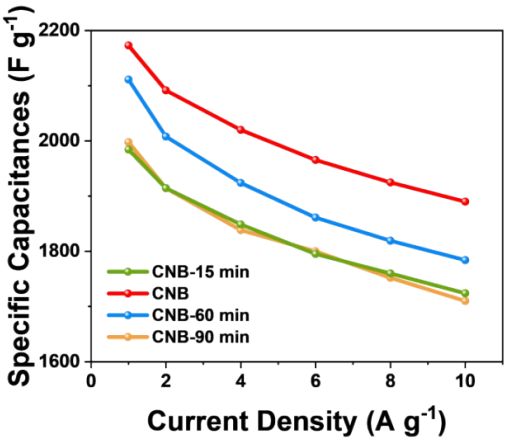

Figure S18. The specific capacitance at different charge/discharge current densities of the CNB, CNB-15 min, CNB -60 min, CNB -90 min.

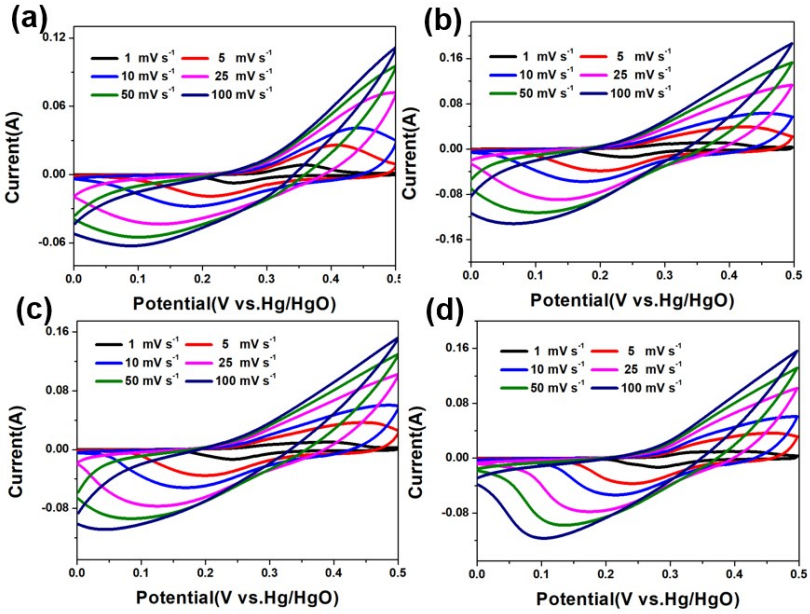

Figure S19. The CV curves of (a) CNB-0 M; (b) CNB-0.2 M; (c) CNB-0.6 M; (d) CNB-0.8 M.

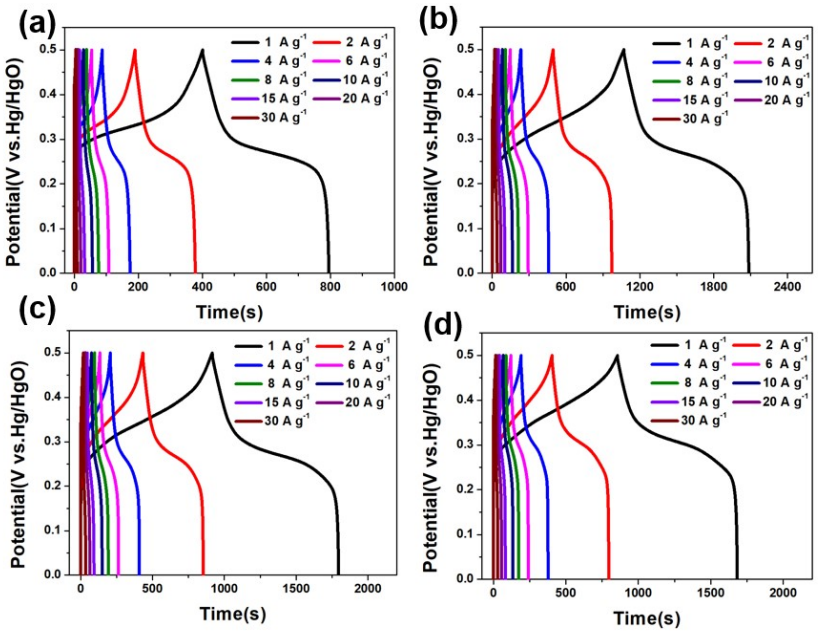

Figure S20. The GCD curves of (a) CNB-0 M; (b) CNB-0.2 M; (c) CNB-0.6 M; (d) CNB-0.8 M.

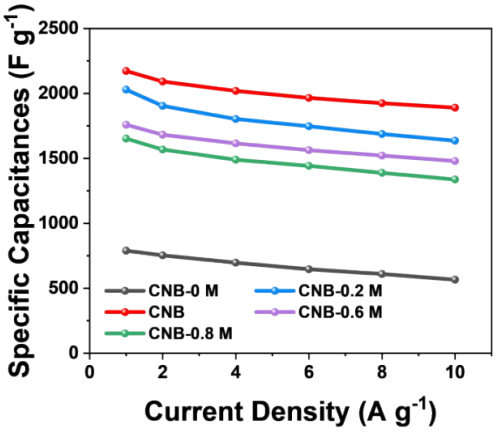

Figure S21. The specific capacitance at different charge/discharge current densities of the CNB, CNB-0 M, CNB-0.2 M, CNB-0.6 M, CNB-0.8 M.

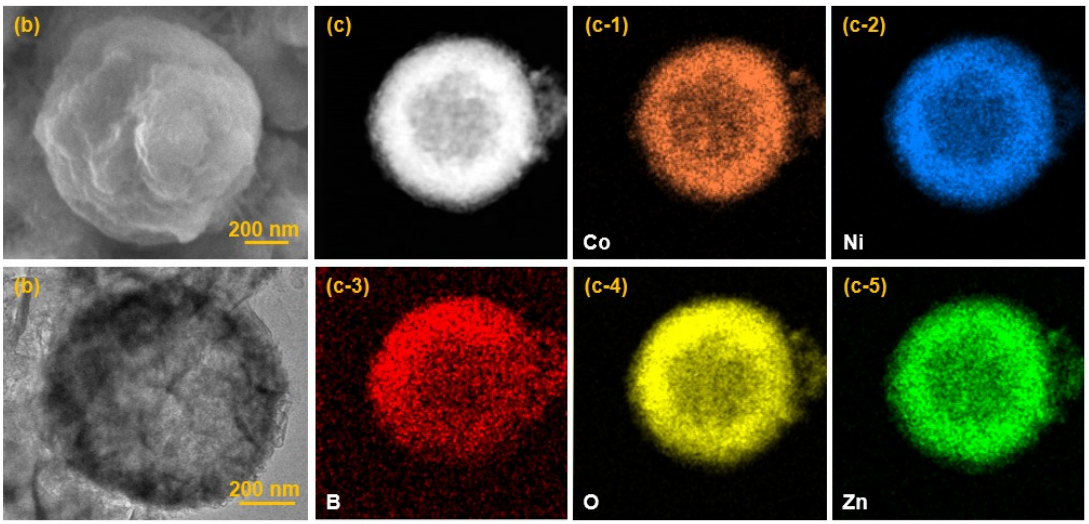

Figure S22. (a) The SEM; (b) the TEM; (c) the TEM-Mapping images of the CNB sample after cyclic stability.

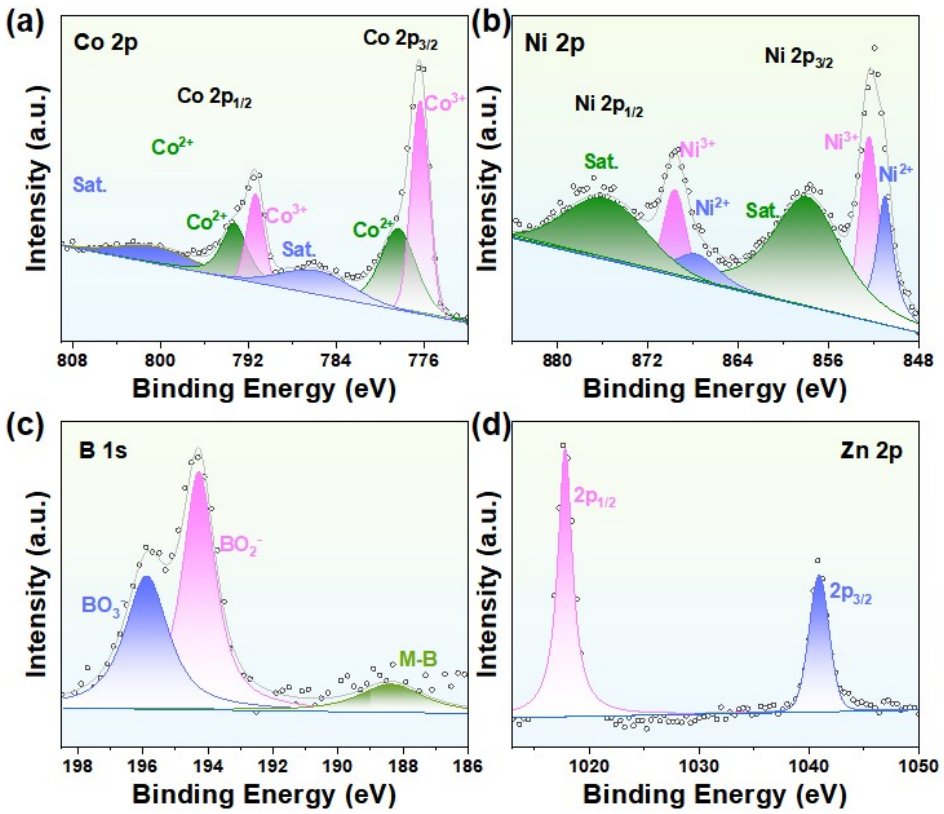

Figure S23. XPS spectra of (a) Co 2p,; (b) Ni 2p; (c) B 1s, and (d) Zn 2p of CNB after the electrochemical cycle test.

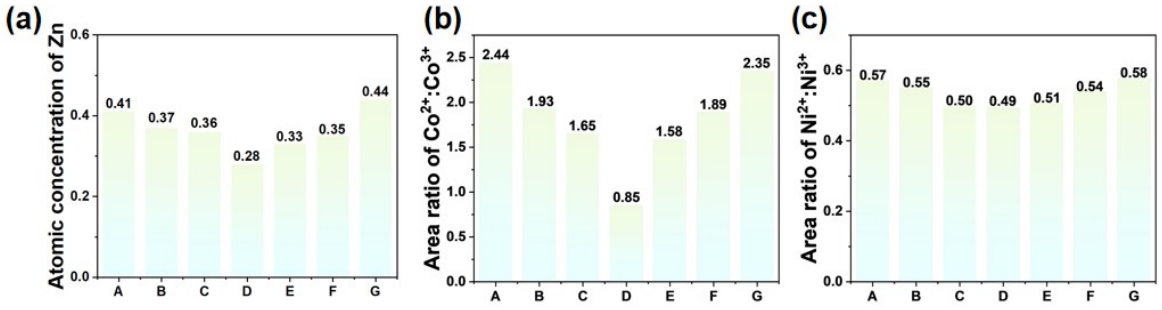

Figure S24. (a) The atomic concentration of Zn content calculated by internal standard Co element. (b) the area ratio of Co^{2+}:Co^{3+}; (c) the area ratio of Ni^{2+}:Ni^{3+} calculated by *ex-situ* XPS.

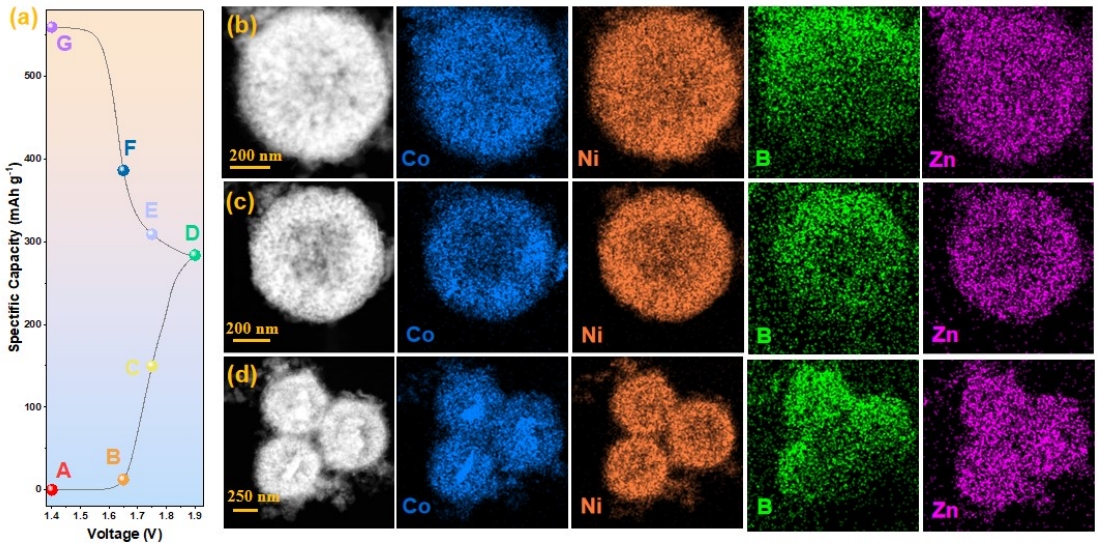

Figure S25. The energy storage mechanism of CNB//rGO-Zn aqueous Zn-based battery. (a) the charge/discharge curves after the rate test; (b-d) the *ex-situ* TEM-mapping analysis at points A, D, and G.

Equation:

The OH^- diffusion coefficient (D) was calculated using the equation

$$D=\frac{R^2T^2}{2A^2n^4F^4c^2\sigma^2} \quad \text{(S-1)}$$

where D is the apparent diffusion coefficient of OH^- ($cm^2\ s^{-1}$), R is ideal gas constant (8.314 J $mol^{-1}\ K^{-1}$), T is Kelvin temperature (K), A is the surface area of the tested electrode (cm^2), n represents the number of electrons per reaction species, F is Faraday's constant (96500 C mol^{-1}) ,c is electrolyte concentration, σ is warburg coefficient.

$$i = av^b \quad \text{(S-2)}$$

Where v is scan rate (mV s^{-1}), i is peak current (A), a and b are constant.

$$i = k_1v^{1/2}{}_+k_2v \quad \text{(S-3)}$$

Where i and v stand for the peak current density and scan rate, respectively. Generally, $k_1v^{1/2}$ and k_2v are associated which the bulk process contribution and the surface process contribution of the peak current density, respectively.

$$E = \frac{I}{m}\int_{t_2}^{t_1} V \quad \text{(S-4)}$$

Where E is the energy density (Wh kg^{-1}), and V is the potential range (V).

$$P = \frac{E}{\Delta t} \quad \text{(S-5)}$$

Where P is the powerty density (kW kg^{-1}), E is the energy density (Wh kg^{-1}), Δt is the discharging time (s).

Table:

Table S1. Parameters of the proposed equivalent circuit model.

Elements / Samples	Rs (Ω)	Rct (Ω)	CPE-P	W-R (Ω)
NB	0.70	0.51	0.47	0.81
C_1N_9B	0.78	0.29	0.91	0.69
C_2N_8B	0.72	0.40	0.86	0.90
CNB	0.55	0.17	0.97	0.93
C_4N_6B	0.86	0.43	0.91	2.79
C_5N_5B	0.74	0.54	0.84	2.19
CB	0.81	0.24	0.98	0.77

Table S2. Atomic concentration of ex-situ XPS spectra of Co, Ni and Zn

Atomic concentration	**Co**	Ni	**Zn**
A	4.66	9.62	1.92
B	3.88	6.94	1.43
C	1.36	4.42	0.49
D	3.58	6.63	0.99
E	2.89	7.18	1.00
F	4.47	2.3	1.46
G	3.13	6.60	1.39